

# CONCATENATION AND REBINNING OF IUE HIGH RESOLUTION SPECTRA

Enrique Solano<sup>1</sup>

<sup>1</sup>INSA. ESA-IUE Observatory. P.O. Box 50727. 28080 Madrid (Spain).

## Abstract

IUE High Resolution spectra will be available in the IUE Final Archive as concatenated spectra. The concatenation procedure is presented here. A study on the degradation of High Resolution spectra to Low Resolution to make both sets of data directly comparable is also shown. Quality flags and errors associated to the rebinned spectra are defined.

Key words: High Resolution spectra; concatenation; rebinning.

## 1 INTRODUCTION

The degradation of High Resolution data to Low Resolution data is a crucial step for many studies, in particular for those based on observations in both dispersion modes. Two problems arise in the process of rebinning from High Resolution data to Low Resolution data: Firstly, the order concatenation in the overlapping spectral regions must be defined. Secondly, the starting wavelength and stepsize of the rebinned spectra must coincide with those of the INES Low Resolution spectra: In NEWSIPS, the wavelengths scales of High and Low Resolution data differ not only because of the spectral resolution (which is order-dependent in High Resolution) but also because of the different wavelength of the first calibrated pixel which, in Low Resolution spectra depends on the NEWSIPS version and the Intensity Transfer Function used (this only for the LWR camera). In this study the procedure used to solve these problems is presented.

## 2 ORDER CONCATENATION

Two criteria have been considered in the definition of the cut wavelength: the S/N ratio of the overlapping wavelength region should be maximized and the order edges, where the ripple correction may be less efficient (Figure 1, order 93), should be avoided. To estimate the S/N ratio of the overlapping region, spectra of IUE standard stars have been used (Tables 1-6). Whenever possible, spectra of BD+28 4211, WD 0501+52 and CD-38 10980 were used since the absence of spectral lines in these stars makes them optimum indicators of the S/N ratio by simply taken the standard deviation of the flux. In all cases

the overlapping region was divided in four regions and the standard deviation of the flux of the two adjacent orders measured. Only non-flagged pixels were used to estimate the S/N ratio as well as to define the size of the overlapping region.

From this study it was deduced that for the LW cameras the S/N ratio is higher in the  $m^{th}$  order than in the  $(m - 1)^{th}$  order in the first two thirds of the overlapping region. Conversely, for the SWP camera the S/N ratio of the  $m^{th}$  order is higher only in the first third of the overlapping region. According to this, the cut wavelength for a given order has been defined as follows:

- **SWP**

$$\lambda_c = \lambda_s + (\lambda_e - \lambda_s)/3. \quad (1)$$

- **LWP, LWR**

$$\lambda_c = \lambda_s + 2 * (\lambda_e - \lambda_s)/3. \quad (2)$$

where

- $\lambda_c$ : cut wavelength
- $\lambda_s$ : starting wavelength ( $(m - 1)^{th}$  order)
- $\lambda_e$ : ending wavelength ( $m^{th}$  order)
- $\lambda_e - \lambda_s$ : size of the overlapping region

The relations given above are valid for all orders except for  $m = 125$  (LWP) and  $m = 120-125$  (both included) (LWR). For these orders it was seen that the S/N ratio of the  $m^{th}$  order was higher than for the  $(m - 1)^{th}$  even beyond the cut wavelengths given by (1) and (2). In these cases all calibrated pixels of the  $m^{th}$  order were considered.

An statistical analysis on the repeatability of the cut wavelengths so defined was also performed. It showed that the standard deviation of the cut wavelength from the mean position is less than  $0.2 \text{ \AA}$  irrespective of the camera and aperture. This allows to define the cut wavelength as a function of the order number ( $m$ ) by the following expressions:

- **LWP**

$$\lambda_{cut} = -7.9697 + 233257.6280/m \text{ (Large aperture)} \quad (3)$$

$$\lambda_{cut} = -7.7959 + 233382.6450/m \text{ (Small aperture)} \quad (4)$$

$$124 \geq m \geq 77$$

- **LWR**

$$\lambda_{cut} = -11.3459 + 233737.5903/m \text{ (Large aperture)} \quad (5)$$

$$\lambda_{cut} = -11.2214 + 233876.9950/m \text{ (Small aperture)} \quad (6)$$

$$119 \geq m \geq 76$$

- **SWP**

$$\lambda_{cut} = 24.3952 + 132875.4838/m + 325840.9715/(m * m) \text{ (Large aperture)} \quad (7)$$

$$\lambda_{cut} = 22.2095 + 133293.4862/m + 300351.2209/(m * m) \text{ (Small aperture)} \quad (8)$$

$$120 \geq m \geq 73$$

For orders that do not overlap ( $m \leq 76$  (LWP),  $m \leq 75$  (LWR) and  $m \leq 72$  (SWP)), only photometrically corrected pixels ( $\nu > -16384$ ) were considered. Since the concatenated spectrum is defined only in the absolutely flux calibrated interval (1150-1980 for the SWP and 1850-3350 Å for the LW cameras), orders out of this range were not considered. Once the spectral orders have been concatenated, the wavelength scale corrections (Cassatella & González (1998), Loiseau et al. (1998)) are implemented. The concatenated spectrum will therefore consists of four columns, namely, corrected wavelength, absolute flux, flux errors (in absolute units) and quality flags. To transform the errors given in the MXHI spectrum (in FN units) to flux units ( $\text{erg/cm}^2/\text{s}/\text{\AA}$ ) they must be multiplied by the ratio of the absolutely calibrated flux to the net flux. Examples of concatenated spectra (black line) are given in Figures 1-3.

Comparing the cut wavelengths calculated by the relations given above, it can be seen that, as expected from the camera geometry, the cut wavelength for the Large aperture is systematically shorter than for the Small aperture for both LW cameras and conversely for the SWP camera. It can be also noticed that, unlike the LW cameras, a quadratic relation is necessary for the SWP camera. The reason for this is the presence of uncalibrated pixels at the red edge of every order. The number of these pixels is maximum at  $m = 125$  decreasing with order number. From  $m = 81 \pm 2$  onwards, all pixels within the photometrically corrected region are flux calibrated. This varying number of uncalibrated pixels introduces a non-linear term in the relation between the size of the overlapping region and order number which affects the definition of the cut wavelength.

### 3 REBINNING

The wavelengths of the rebinned spectrum have been set according to the following expression:

$$\lambda_i = \lambda_{start} + (i - 1) * step \quad (9)$$

where

- $\lambda_i$ : Wavelength of  $i - th$  pixel.
- $\lambda_{start}$ : Wavelength of the first calibrated pixel (consistent to INES Low Resolution spectra).
- **step**: 2.6693 Å/pixel (LW cameras), 1.6764 Å/pixel (SWP camera).

Defining the binsize as **step**, the edges of a bin centered at  $\lambda_i$  will be:  $\lambda_i - step/2$ ,  $\lambda_i + step/2$ . The rebinning from HiRes to LoRes has been performed in such a way that the total flux

is conserved, that is, if  $n$  pixels with fluxes  $f_1, f_2, \dots, f_n$  are rebinned into one, the total flux in the bin will be

$$TotalFlux = \sum_{i=1}^{i=n} (\lambda_i - \lambda_{i-1}) * (f_i + f_{i-1})/2. \quad (10)$$

where the flux at the bin edges ( $i=1, i=n$ ) is calculated by linearly interpolating between the two adjacent pixels. Finally, the associated value to the resulting pixel will be

$$flux = TotalFlux/step \quad (11)$$

### 3.1 FLUX CONSERVATION

To ensure the flux conservation after rebinnning, LoRes and rebinned HiRes spectra of BD+28 4211 have been compared. Figure 4 compares the averaged spectra of 88 Low Resolution and 38 High resolution SWP spectra showing an excellent agreement.

A further test on the flux conservation was performed by measuring the equivalent widths of emission lines of a sample of High Resolution RR Tel spectra. Only non-flagged lines were considered in the analysis. Differences of less than 10% in the ratio between the equivalent widths of the lines of the High Resolution and rebinned spectra were achieved, differences that can be explained by the uncertainty in the local continuum placement of the rebinned spectra. This is confirmed when synthetic noiseless spectra are used in the analysis.

### 3.2 FLAGGING

The quality flags denote exceptional conditions in the data in such a way that the more serious conditions have more negative values. These quality flags are encoded to indicate all problem conditions associated with each pixel. For the rebinned spectra, only a subset of the original NEWSIPS flagging conditions are considered, namely

- **-8192:** Missing minor frames in extracted spectrum
- **-1024:** Saturated pixel
- **-16:** Microphonic noise (LWR only)
- **-8:** Potential DMU corrupted pixel
- **-2:** Uncalibrated data point

Pixels flagged with other quality flags are not taken into account in the rebinning process.

### 3.3 ERRORS

An important point to be noticed when working with High and Low Resolution spectra is the different meaning of the error vectors due to the different extraction method used in each case: whereas in Low Resolution (optimal extraction) the errors associated to the flux at wavelength  $\lambda$  are given by (12), in High Resolution (boxcar extraction) they are calculated using (13).

$$\text{error} = \sqrt{1/\sum p(i)^2/\sigma(i)^2} \quad (12)$$

$$\text{error} = \sum |\sigma(i)| \quad (13)$$

where  $p(i)$  and  $\sigma(i)$  are the corresponding spatial profile and estimated noise values of the  $i$ -th pixel at wavelength  $\lambda$ . Moreover, the errors in High Resolution are given in FN units. To transform them to flux units ( $\text{erg}/\text{cm}^2/\text{s}/\text{\AA}$ ), the errors should be multiplied by the ratio of the absolutely calibrated flux to the net flux.

For the rebinned spectra, the errors have been calculated according to the following formulae:

$$\text{error} = \sqrt{\sum e_i^2/n} \quad (14)$$

where  $e_1, e_2, \dots, e_n$  are the calibrated errors ( $\text{erg}/\text{cm}^2/\text{s}/\text{\AA}$ ) of the  $n$  pixels rebinned into one.

## 4 CONCLUSIONS

A study on the concatenation and degradation of High Resolution to Low Resolution spectra has been performed. The order concatenation was made taking into account the following two criteria: the S/N of the overlapping regions must be maximized and the order edges, where undesirable ripple effects may be present, must be avoided. The rebinning has been defined in such a way that ensures the flux conservation within the bin: different tests have proved that both the flux distribution and the equivalent width of the lines are conserved after rebinning. The flagging criteria used in NEWSIPS have been used to denote abnormal conditions in the rebinned spectra although only a subset of the original list of flags has been considered. Also, and because of the different spectral extraction procedures implemented in Low Resolution (optimal extraction) and High Resolution (boxcar extraction), the errors in the rebinned and LoRes spectra have a different definition and this must be kept in mind when working with Lores and rebinned HiRes data.

## References

- [1] Cassatella A., González Riestra R., 1998, *Evaluation of IUE High Resolution spectra processed with NEWSIPS*, INES Document 3.7
- [2] Loiseau N., Pérez Calpena A., González Riestra R., 1998, *INES Data Description*, INES Document 4.1

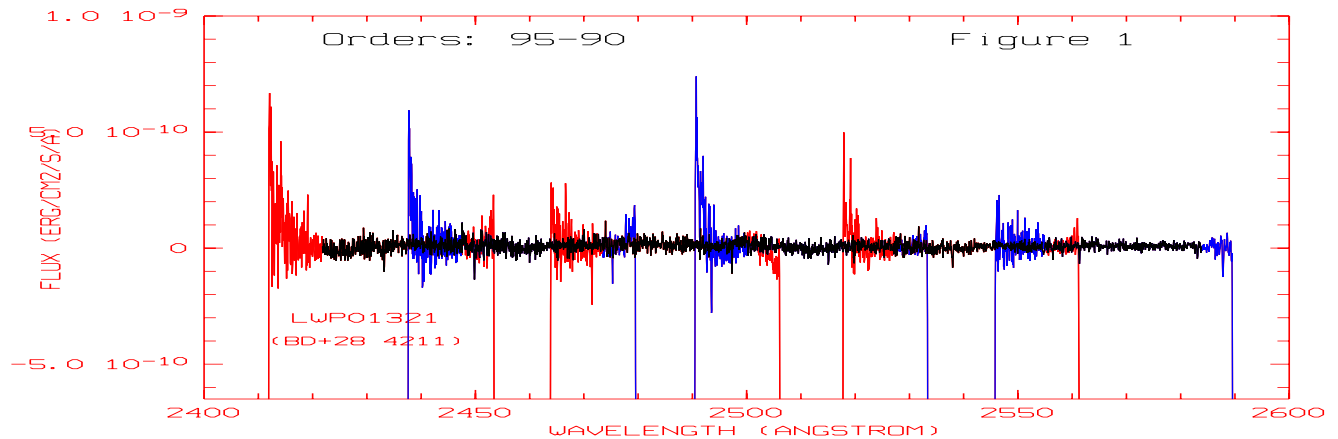


Figure 1: Concatenated spectrum (LWP camera)

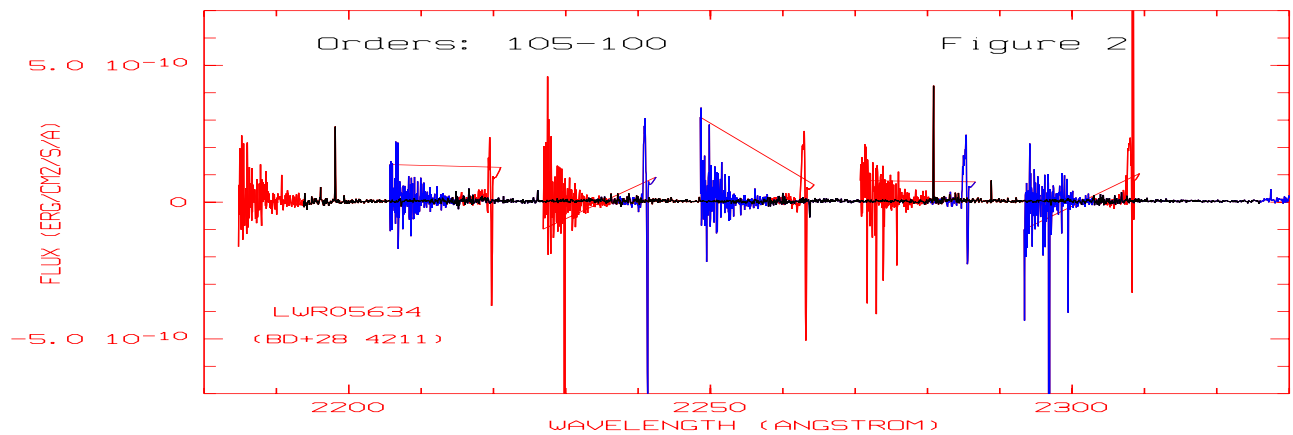


Figure 2: Concatenated spectrum (LWR camera)

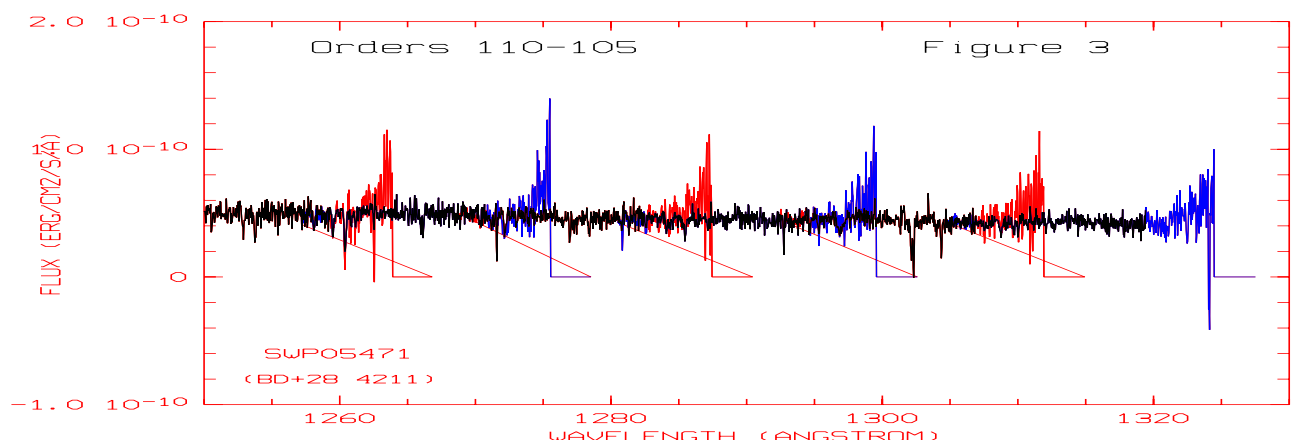


Figure 3: Concatenated spectrum (SWP camera)

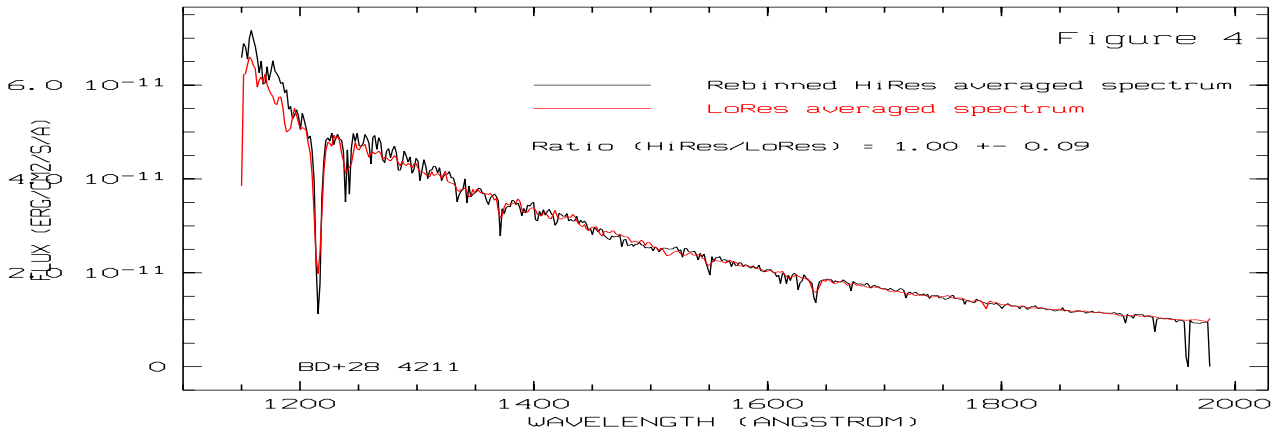


Figure 4: Comparison between rebinned High Resolution and Low Resolution spectra.

Table 1: List of image numbers. (LWP camera, Large aperture)

BD+28 4211								
01321	08392	11578	13776	17977	19302	23452	26036	28494
01441	08435	11580	13777	17978	19460	23622	26037	28717
01461	09703	12059	15685	18021	19461	23682	26057	28767
01749	09726	12060	15686	18121	21336	24252	26176	28938
01767	10835	12297	16983	18800	21390	25639	26181	29020
06961	10881	12356	17002	19290	21638	25903	26316	29111
08228	11292	13303	17003	19291	23377	25926	26675	29165
CD-38 10980								
05725	20114	20279	21058	25084	26102	27865	27920	28786
20113	20120	21045						
WD0501+52								
19999	20078	24189	24608	29375	29442			

Table 2: List of image numbers. (LWP camera, Small aperture)

HD 149438	HD 93308	HD 20902	HD 39801	HD 48915	HD 62509	HD 21071	HD 172167
01965	03115	02909	04098	03119	02913	02912	03008
01979	03116	03009	04250	03120	02914		
02725	03974						
03691	03975						

Table 3: List of image numbers. (LWR camera, Large aperture)

BD+28 4211							
05024	05469	05470	05471	05634	17222	18473	18483

Table 4: List of image numbers. (LWR camera, Small aperture)

HD 120315			HD 3360	HD 34816	HD 149881	HD 60753	BD+28 4211
01545	02518	04487	01468	02032	01690	01973	01491
01752	03076	04875	01621	02890	04898		
01928	03077	04903	01831	02891			
02125	03345	05070	02554	05728			
02226	03479	05540	04648				
02331	03767	05999	06819				
02515	04202	06506					

Table 5: List of image numbers. (SWP camera, Large aperture)

BD+28 4211									
05471	28519	31123	36429	39298	43010	48262	51590	52277	
05778	28607	31429	37202	40209	45012	48263	51789	52278	
05779	29114	31809	37292	40219	45085	48285	51863	52345	
06305	29783	32286	37878	40440	45159	48406	52048	52694	
06306	29869	32534	37898	40441	45266	48409	52098	55006	
11127	29911	32587	38862	41996	46122	48587	52196	55391	
16068	29925	33766	38863	42103	47778	49068	52234	55692	
18880	31069	34009	38948	42556	48120	51240	52267	55693	
26964	31094	36395	39103	42602	48261				
CD-38 10980									
18290	40922	41379	41466	41495	42297	47010	48308	51681	
25669	41346	41435	41467	42260	42309	47273	50517	51794	
WD0501+52									
18217	41183	41281	46600	46677	46693	52405	52677	55664	
22428	41207	41301							

Table 6: List of image numbers. (SWP camera, Small aperture)

HD 3360			HD 93521	HD 149881	HD 34816	HD 60753	BD+28 4211
01481	02022	05409	01607	01810	02250	02191	01542
01482	02885	05469	04076	03967	03279		
01483	03712	05470	05620	04072	07477		
01484	03906	07806	05621	05648	15605		
01722	05261	08133	05657	05649	53827		
01724	05408	23862	33179				